Nano-Structures & Nano-Objects

Titanium Dioxide/Nitrogen-Doped Graphene-Biopolymer Based Nanocomposite Films for Pollutant Photodegradation and Laser Desorption Ionization Mass Spectrometry of Biomarkers

--Manuscript Draft--

Manuscript Number:	NANOSO-D-24-00096R1
Article Type:	Research Paper
Keywords:	titanium dioxide; Nitrogen-doped graphene; Nanocomposite film; Photodegradation; LDI-MS
Corresponding Author:	Nadnudda Rodthongkum Chulalongkorn University THAILAND
First Author:	Tatiya Siripongpreda
Order of Authors:	Tatiya Siripongpreda
	Noppakhate Jiraborvornpongsa
	Russell J. Composto
	Nadnudda Rodthongkum
Manuscript Region of Origin:	Asia Pacific
Abstract:	Titanium dioxide (TiO2)/nitrogen-doped graphene (NG) nanocomposite is prepared via a solvent-free hydrothermal reaction. The resulting TiO2/NG materials exhibit a reduction of the band gap energy compared to pristine TiO2 from 3.27 eV to 2.69 eV. These materials are characterized by scanning transmission electron microscopy (STEM), energy dispersive X-ray spectroscopy (EDX), and X-ray photoelectron spectroscopy (XPS). To prepare biopolymer films with photocatalytic properties, TiO2 and NG are mixed with biodegradable chitosan and spin-coated on a silicon wafer. Film roughness and thickness are evaluated by atomic force microscopy (AFM). These films are then tested for ciprofloxacin photodegradation by irradiating with visible light. In comparison to the TiO2/chitosan films, the addition of NG substantially enhances photodegradation efficiency by up to 34% upon the addition of 5% w/w of NG. Furthermore, this film is shown to be a good substrate for biomarker detection using laser desorption ionization mass spectrometry (LDI-MS). In summary, this nanocomposite-biopolymer film provides good photocatalytic activity towards ciprofloxacin degradation and enhances the ionization efficiency of peptide biomarkers in LDI-MS owing to high efficiency of laser absorption/desorption. This nanocomposite film might be useful for environmental-related and medical application.
Suggested Reviewers:	Akira Nakajima anakajim@ceram.titech.ac.jp
	Todd Emric tsemrick@mail.pse.umass.edu
	Christopher Li chrisli@drexel.edu
Opposed Reviewers:	
Response to Reviewers:	

Cover Letter

Nadnudda Rodthongkum, Ph.D.
Metallurgy and Materials Science Research Institute
Chulalongkorn University, Bangkok 10330 Thailand
Phone: +66(0)2 218-4233 Fax: +66(0)2 611-7586
E-mail: Nadnudda.R@chula.ac.th

February 17th, 2024

Dear Editor,

On behalf of the authors, I am writing to submit our manuscript entitled, "Titanium Dioxide/Nitrogen-Doped Graphene-Biopolymer Based Nanocomposite Films for Pollutant Photodegradation and Laser Desorption Ionization Mass Spectrometry of Biomarkers" by Tatiya Siripongpreda, Noppakhate Jiraborvornpongsa, Russell J. Composto, and Nadnudda Rodthongkum to be considered for publication as a research article in ***Nano-Structures & Nano-Objects***.

This manuscript describes a nanocomposite-biopolymeric film based on nano-sized titanium dioxide/nitrogen-doped graphene nanocomposite (TiO_2/NG) for using in photodegradation, and laser desorption-ionization mass spectrometry (LDI-MS). The TiO_2/NG was composited using hydrothermal reaction to form nano-sized TiO_2/NG nanocomposites to minimize surface light reflection and improve catalytic efficiency. Then, the nanocomposite nanoparticles were integrated with chitosan (CH) support and spin-coated onto a silicon wafer to fabricate TiO_2/NG-CH thin films. These films were applied for ciprofloxacin photodegradation and applied as a solid matrix for LDI-MS detection of peptide biomarkers at trace level with high sensitivity (*e.g., angiotensin II, angiotensin I, bombesin, ACTH, and somatostatin 28*).

From these satisfactory results, it was concluded that the developed TiO_2/NG-CH thin films can be considered as an alternative material that is potentially integrated and utilized for diverse applications, including, environmental and biomedical application (e.g., pollutant removals and biomarker detection).

We confirm that this manuscript is submitted to ***Nano-Structures & Nano-Objects*** and has not been published elsewhere, and it is not under consideration for publication in other journals.

We hope that with the information provided, our revised manuscript is ready to undergo the peer review process. In case that you have any question, please feel free to contact me at any time.

Sincerely,

Nadnudda Rodthongkum

Nadnudda Rodthongkum, Ph.D.
Research Professor

Highlights

- TiO_2/NG nanocomposite is successfully synthesized and it can reduce the band gap of pristine TiO_2.
- TiO_2/NG-chitosan nanocomposite thin film is fabricated for pollutant photodegradation and LDI-MS detection of biomarkers.
- The nanocomposite film shows higher efficiency for ciprofloxacin photodegradation compared with NG-CH and TiO_2-CH films.
- The nanocomposite film offers high laser absorption/desorption and it is applied as a substrate for LDI-MS detection of biomarkers.

Graphical abstract

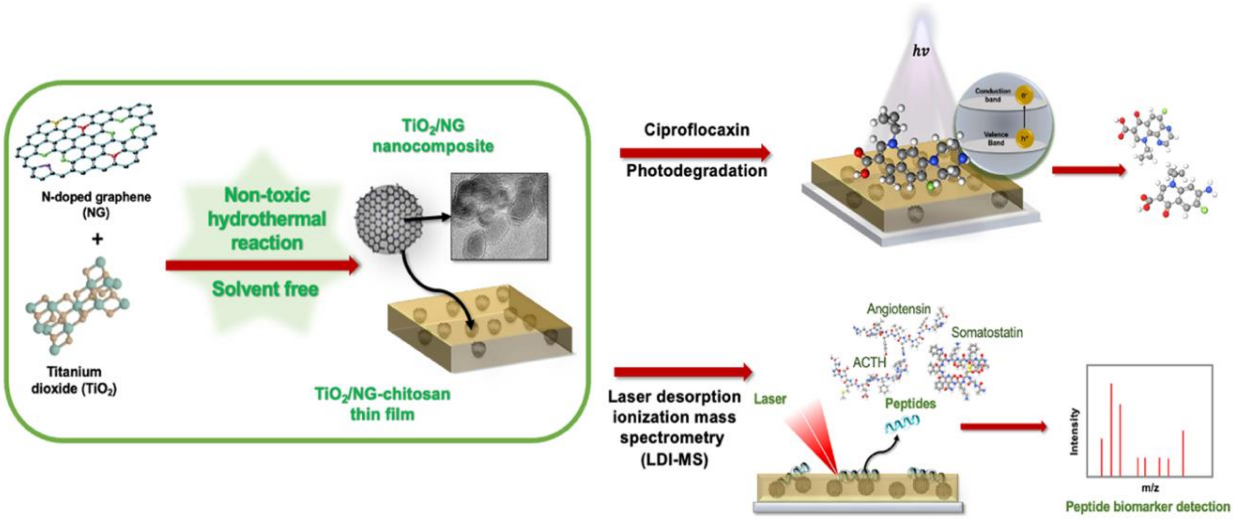

Manuscript Number: NANOSO-D-24-00096
Title: Titanium Dioxide/Nitrogen-Doped Graphene-Biopolymer Based Nanocomposite Films for Pollutant Photodegradation and Laser Desorption Ionization Mass Spectrometry of Biomarkers

Thanks to the editor and the reviewers for the useful comments and suggestions. The authors have addressed each point raised by the editor and the reviewers (in red). Also, we have included more information and modified the revised manuscript as highlighted.

Editor and Reviewer comments:
Add some more recent updates in the literature review of the year 2024.
We have already added more information, cited and updated references in the revised manuscript (Introduction section: Line 7 Page 3, Line 21-22 Page 3, Line 34 Page 4, Line 37 Page 4, and Line 49-51 Page 5).

Reviewer #1: Improve the discussion of your results to make the contribution clear.
We have already improved the discussion by rephrasing sections throughout the manuscript and incorporating the additional details into the revised version to clarify the results.

Reviewer #2:
Major revision is needed for acceptance of this article.
Thorough English revision is recommended to improve the quality of this article
This revised version of a manuscript is corrected by a native English speaker (Prof. Russel Composto).

Minor corrections
XPS model and make are missing band gab value
We have provided XPS model and UV-Vis-NIR spectrophotometer model in Section 2.3.

Fig. 8 displayed….displays
Conclusions
CH power (powder)
We have corrected these grammatical errors in the revised manuscript.

Major corrections are the following
Quality of XPS graphs need to be improved. Peak fitting of Ti is wrong. (>ti doublet, so peak fitting should be applied in both peaks.
We have improved the quality of the graphs and included the edited versions in the revised manuscript, and we also have already re-conducted peak fitting for Ti in the manuscript.

In general, all graphs qualities are very poor. Need to limit the Y scale maximum (scale expanded) and plot the lines clear and well (different types of lines or line plus symbol option)
We have improved quality of the graphs and figures (Fig. 1, Fig. 3, Fig. 4, Fig. 5, Fig. 6 and Fig. 7) in the revised manuscript.

TiO_2 presented large aggregates (**Fig. 4b**).. some wrinkles (**Fig. 4c**)… nanocomposites (**Fig. 4d – 4f**).. All are part of Figure 1.
We have corrected the errors pointed out by the reviewer in the revised manuscript.

Chemical states of c in TiO_2 lattice ?? what it means??

We have corrected the mentioned error from "chemical states of c in TiO_2 lattice" to "chemical states of O^{2-} in TiO_2 lattice, hydroxyl groups and O^{2-} from water absorption on TiO_2 surface" in the revised manuscript (Page 12).

A Raman spectral analysis could be really useful in confirming the nanocomposite formation.

As suggested by the reviewer, raman spectral analysis was carried out to confirm the formation of the nanocomposite. As illustrated in the raman spectra below, The main peaks of the pristine NG spectra was 1346.88 and 1589.51 cm^{-1} which correspond to disordered (D band) and graphitic ordered (G band) structures, respectively. The spectrum of TiO_2/NG displyed significant raman peaks at 147.03, 397.35, 516.72, and 641.06 cm^{-1} from TiO_2 and two prominent peaks at 1352.88 and 1601.17 cm^{-1}. It was found that peaks of D and G bands and the ratio between the intensities of D and G bands (I_D/I_G) indicating defect density in the graphitic structure of NG and TiO_2/NG was different. Moreover, D and G bands of the pristine were shifted when composited with TiO_2 using hydrothermal treatment. This can confirm the formation of the TiO_2/NG nanocomposite.

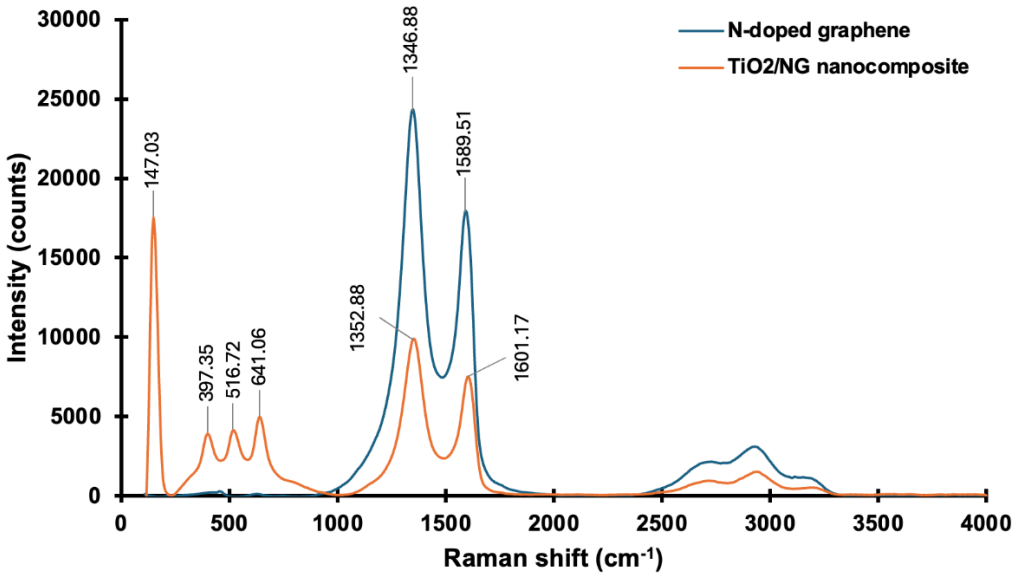

Furthermore, the formation of the nanocomposite was confirmed by using elemental mapping and XPS, which are illustrated in Fig. 2 and Fig. 3, respectively.

The nanocomposite films were exposed to ciprofloxacin solution to investigate the degradation of CH, TiO2-CH, NG-CH and TiO2/NG-CH thin films. The aim was to study degradation of the films or degradation of ciprofloxacin???

The main purpose of this work was to study the potential of TiO_2/NG-CH thin films for ciprofloxacin degradation. The polymeric films degradation was examined to investigate the dispersity of nanomaterials within the CH carrier, and an opimal exposure time for ciprofloxacin degradation experiment.

Titanium Dioxide/Nitrogen-Doped Graphene-Biopolymer Based Nanocomposite Films for Pollutant Photodegradation and Laser Desorption Ionization Mass Spectrometry of Biomarkers

Tatiya Siripongpreda [a, b], *Noppakhate Jiraborvornpongsa* [b, c], *Russell J. Composto* [d*], *Naddudda Rodthongkum* [b,e*]

[a] Nanoscience and Technology Interdisciplinary Program, Chulalongkorn University, Phayathai Road, Wangmai, Patumwan, Bangkok 10330, Thailand

[b] Metallurgy and Materials Science Research Institute, Chulalongkorn University, Phayathai Road, Wangmai, Patumwan, Bangkok 10330, Thailand

[c] Photocatalysts for Clean Environment and Energy Research Unit, Faculty of Science, Chulalongkorn University, Phayathai Road, Wangmai, Patumwan, Bangkok, 10330, Thailand

[d] Department of Materials Science and Engineering, University of Pennsylvania, Philadelphia, Pennsylvania 19104, United States

[e] Center of Excellence in Responsive Wearable Materials, Chulalongkorn University, Soi Chula 12, Phayathai Road, Pathumwan, Bangkok, 10330, Thailand

Abstract:

Titanium dioxide (TiO_2)/nitrogen-doped graphene (NG) nanocomposite is prepared via a solvent-free hydrothermal reaction. The resulting TiO_2/NG materials exhibit a reduction of the band gap energy compared to pristine TiO_2 from 3.27 eV to 2.69 eV. These materials are characterized by scanning transmission electron microscopy (STEM), energy dispersive X-ray spectroscopy

(EDX), and X-ray photoelectron spectroscopy (XPS). To prepare biopolymer films with photocatalytic properties, TiO_2 and NG are mixed with biodegradable chitosan and spin-coated on a silicon wafer. Film roughness and thickness are evaluated by atomic force microscopy (AFM). These films are then tested for ciprofloxacin photodegradation by irradiating with visible light. In comparison to the TiO_2/chitosan films, the addition of NG substantially enhances photodegradation efficiency by up to 34% upon the addition of 5% w/w of NG. Furthermore, this film is shown to be a good substrate for biomarker detection using laser desorption ionization mass spectrometry (LDI-MS). In summary, this nanocomposite-biopolymer film provides good photocatalytic activity towards ciprofloxacin degradation and enhances the ionization efficiency of peptide biomarkers in LDI-MS owing to high efficiency of laser absorption/desorption. This nanocomposite film might be useful for environmental-related and medical application.

Graphical abstract

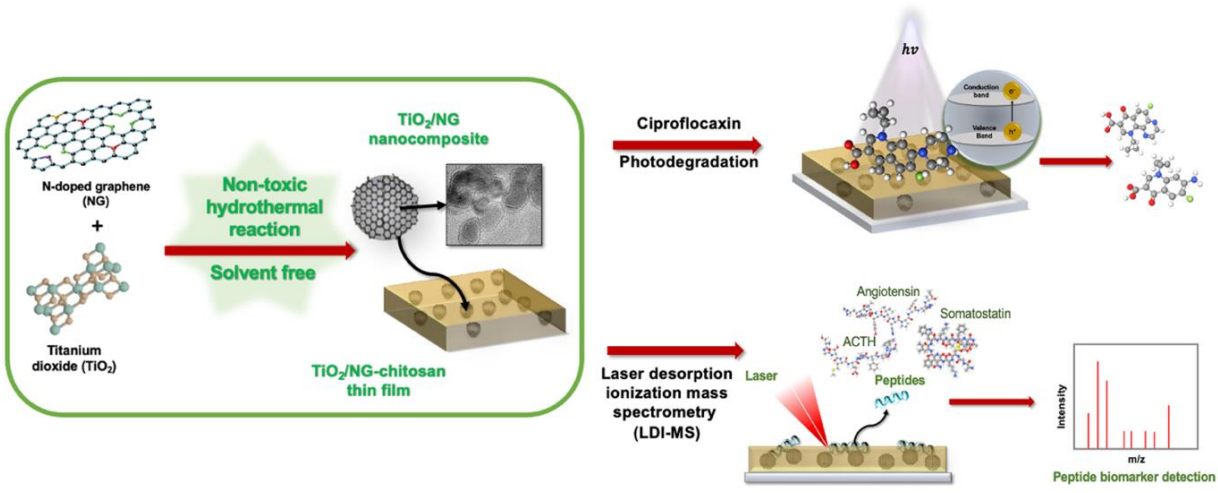

Keywords

Titanium dioxide, Nitrogen-doped graphene, Nanocomposite film, Photodegradation, LDI-MS

1. Introduction

The rapid growth of industrialization and population has led to significant environment challenges across the globe. The degradation of pollutants can play an important role in mitigating the impacts of pollutant contamination while improving environment conditions particularly in areas such as clean water, where photocatalysis can play an important role in facilitating the degradation or breakdown of harmful pollutants. To prepare photocatalyst for such processes, a solvent-free hydrothermal reaction is an attractive approach because it uses benign chemicals, is economical, and has been shown to efficiently separate solid products [1-3].

Titanium dioxide (TiO_2) is a wide band gap metal oxide semiconductor commonly used as a photocatalysis [4] due to its strong oxidizing ability, chemical stability, low cost, and non-toxicity [5]. There are three forms of TiO_2 including anatase, rutile, and brookite which consist of interconnected TiO_2 octahedra with different degrees of distortion [6]. Anatase offers the highest stability in the nanoscopic scale with high photocatalytic activity over rutile; however, anatase has a wider band gap energy [7]. To reduce band gap energy of semiconductors, doping impurities can induce intraband energy states and narrow of the band gap of pristine semiconductors to allow compatibility with visible light [8]. Moreover, thermal treatments, such as annealing, of some semiconductor materials (*e.g., TiO_2*) critically affects electrical properties by decreasing their band gap energy [9]. Graphene is an allotrope of carbon in the form of a single layered hexagonal lattice with sp^2 hybridization having high conductivity, high stability, and a large specific surface [10]. Doping nitrogen atoms into graphitic structure to create nitrogen-doped graphene (NG) provides functional groups, catalytic activity, with increased free carrier density [11, 12]. NG also exhibits high electronegativity that promotes adsorption property and electron transportation [13]. Since NG is graphitic structured material; NG displays and high electron mobility [14] indicating NG is

a promising component for altering electronic property [15-17] and advancing photocatalytic performance of the semiconductors [18]. The addition of NG to TiO_2 is attractive because nitrogen acts as an electron donor and graphene minimizes surface light reflection, enhancing light-material interaction. According to previous reports, graphene-based materials-semiconductors hybrids demonstrated enhancement of light absorption [19], which is related to photocatalytic activity [20-22] and photochemical reaction [23]. Therefore, combining TiO_2 anatase nanoparticles with carbon-based structures can potentially reduce band gap value of the TiO_2 since NG has outstanding light absorption [24], and nitrogen dopant demonstrates the ability to reduce the original band gap or to generate localized states in the band gap [25, 26]. Thus, NG is selected to composite with TiO_2 nanoparticles to improve the recombination of photoexcited carriers, improvement in light-material interaction and photocatalytic property of pristine TiO_2 anatase [27] for diverse applications.

Adsorption is one of the effective methods to remove pollutants based on pollutant degradation [28] using biopolymers, for example, chitosan and cellulose, as adsorbents. Chitosan (CH), a bio-derived non-toxic cationic biopolymer, has a charge density that depends on the degree of acetylation and pH of the solvent [29], and is selected for using as a polymeric film support for the nanocomposites prepared by spin-coating since CH possesses biocompatibility, biodegradability and excellent film-forming ability [30]. According to the previous research, CH shows the ability to improve the dispersibility of nanoparticles [31] and CH had excellent physical properties as excellent carriers [32]. The immobilization of nano-catalysts or nanocomposites on a support can alter electronic property [33] allows for improved catalytic efficiency [34], recovery and recycling, and reduces particle leaching.

In addition to its photocatalytic activity, TiO_2 demonstrates great promise as a solid matrix substrate for laser desorption-ionization mass spectrometry (LDI-MS) that substantially increases the ionization efficiency of the organic molecules with low interferences compared with the traditional organic matrices [35]. According to previous research, TiO_2 also demonstrates a high specificity in ability to reversibly bind to phosphates, which is beneficial for applying in the enrichment of phosphorylated peptides and organic phosphates [36]. N-doped graphene having sp^2 hybridization and large specific surface area [37] with abundance of functional groups offers a clearer matrix background, higher salt tolerance, and higher sensitivity compared with other graphene-based materials [38, 39]. According to previous studies, the graphitic structure facilitates integration of molecules onto the surface, and its large surface area enhances the interfacial interaction [40] indicating that NG is suitable for utilizing in LDI-MS. LDI-MS is a high-performance technique used to determine trace amount of chemicals or compounds in complex mixtures. It can be used in monitoring the toxic substances in wastewater [41]. Currently, LDI-MS has become a tool that is capable to detect not only identifying small molecules but also detecting biomarkers and large molecules, and more. This directly provides health assessment and influences overall well-being of the population.

In this study, a nano-sized TiO_2/NG nanocomposite-biopolymer based thin film is a promising solid matrix for biomolecule identification by LDI-MS. The peptide biomarkers are peptides that are capable to indicate diseases [42]. The identification of peptide biomarkers helps diagnosis and therapy of diseases, leading to effective health assessment and disease prediction [43].

Herein, the nano-sized TiO_2/NG nanocomposite was synthesized using a solvent-free method to increase photocatalytic activity via facile hydrothermal reaction to obtain a relatively low band gap TiO_2/NG that can absorb energy in visible range, and laser absorption ability, which the nano-

sized TiO_2/NG nanocomposite can be adapted in coating [44] and numerous photoabsorption-related applications including environmental and medical-related applications. These developed TiO_2/NG-CH thin films are firstly applied for pollutant degradation and as a substrate for LDI-MS detection of large-molecule biomarkers and/or pollutants.

2. Experimental

2.1 Materials and instruments

Titanium dioxide nanopowder (TiO_2, anatase with <25 nm particle size) was purchased from Sigma-Aldrich, USA. Nitrogen-doped graphene (NG) was obtained from ACS material, USA. Chitosan (CH), Chitoclear® Cg-10 (Mw: 60 kDa and degree of deacetylation: 87%) was received from Primex ehf., Iceland. Glacial acetic acid and isopropanol (IPA) were from Fisher scientific, USA. N-type, oriented silicon wafers (dopant Ph, 10−20 Ω·cm resistivity, single side polished) were purchased from Silicon Quest International. Ciprofloxacin hydrochloride was purchased from Selleck Chemicals, USA. Peptide calibration standard II was obtained from Bruker, Germany. The pH meter was purchased from METTLER TOLEDO, USA.

2.2 Synthesis of the titanium dioxide/nitrogen-doped graphene (TiO_2/NG) nanocomposites

TiO_2 nanopowder and varied amount of NG ranging from 0.0 - 15.0% w/w were mixed in with ultrapure water and sonicated for 8 h. Subsequently, the dispersion was added to a 100 mL Teflon-line autoclave and heat-treated at 180°C for 24 h. After the hydrothermal reaction, the obtained nanocomposite suspension was centrifuged at 8000 rpm for 15 min and washed the with ethanol for 3 times. Then, the nanocomposite was dried at 60°C.

2.3 Material Characterization

UV-Vis-NIR spectrophotometer (Varian Cary 5000, Agilent) was used for the determination of absorption spectra. Scanning transmission electron microscope (STEM, JEOL F200) was used for size and morphology observation of nanomaterials and elemental mapping. The particle surfaces were investigated by using a scanning electron microscope (SEM) (Hitachi SU3500 - Horiba X-manX). X-ray Photoelectron Spectroscopy (XPS) (Kratos Analytical Axis UltraDLD) was used to analyze elemental composition of nanocomposites and chemical state. Atomic force microscope (AFM, Bruker Icon) was utilized for nanoparticle analysis and surface roughness measurement.

2.4 Band gap estimation

The synthesized TiO_2/NG nanocomposites were sonicated with DI water for 3 h before filtration with a 0.22 μm filter to eliminate aggregates. TiO_2/NG colloidal solution was determined by measuring its absorbance using UV-Vis-NIR spectrophotometer [45, 46]. Band gap energies of the synthesized nanocomposites were calculated by using Tauc function, which is based on the energy-dependent absorption coefficient (α) that is expressed by eq. 1:

$$(\alpha \cdot h\nu)^{1/\gamma} = B(h\nu - E_g) \quad \text{(eq. 1)}$$

Where h is the Planck constant, ν is the photon's frequency, E_g is the band gap energy, and B is a constant. The γ factor was ½ or 2 for indirect transition band gaps [45].

2.5 Preparation of CH thin films with TiO_2/NG nanocomposites

CH powder was dissolved in a mixture of 50% v/v acetic acid (1.0% v/v) and IPA. TiO_2 or TiO_2/NG nanocomposites (0.075% w/v) were added to the CH solution, sonicated for 3 h and

filtrated with a 0.22 μm filter. The silicon wafer was cut into 1.0 × 1.0 cm^2 and washed with methanol and toluene then, dried with N_2. 50 μL of the prepared solution was dropped onto the silicon wafer and spin-coated using 5000 rpm for 1 min.

2.6 Photocatalytic activity of TiO_2/NG-CH thin film

The photocatalytic degradation of ciprofloxacin was studied under visible light irradiation using a 300 W Xe lamp with a UV cutoff filter. The spin-coated films (CH, TiO_2-CH, NG-CH, TiO_2/NG-CH) with size of 1.0 x 1.0 cm^2 were immersed in 3.0 ml of ciprofloxacin solution with a concentration of 50 mg/mL without adding H_2O_2, and exposed to visible light for 60 min. The concentration of ciprofloxacin solutions before and after exposing to light in the visible range was measured in a range of 300-700 nm by using a UV-Visible spectrophotometer. The photocatalytic efficiency (%) is calculated using the following eq. (2):

$$\text{Efficiency (\%)} = (C_0 - C_e)/C_0 \qquad \text{(eq. 2)}$$

Where C_0 corresponds to initial concentration, and C_e corresponds to final concentration after irradiation [47].

2.7 Laser desorption ionization mass spectrometry (LDI-MS) of CH film with TiO_2/NG

The standard peptide solution (1 μM) was dropped onto the as-prepared spin-coated wafer and dried at a room temperature 25±5 °C prior to attaching to the target plate and inserting into LDI-MS. All LDI-MS experiments were performed on a Bruker Autoflex Max MALDI-TOF mass spectrometer with 30% N_2 laser (337 nm) intensities and 30 laser shots.

3. Results and discussion

3.1 Characterization of TiO_2/NG nanocomposite

The as synthesized TiO_2/NG nanocomposites were characterized by TEM as shown in **Fig. 1a**. prepared using a hydrothermal reaction, a key feature of these nanocomposites are the round TiO_2 particles with a diameter of approximately 20 nm. According to previous research, the high temperature of the hydrothermal reaction is an important factor determining the shape and size of TiO_2 [48].

Furthermore, SEM was used to characterize the pristine TiO_2, nitrogen-doped graphene (NG) and TiO_2/NG nanocomposites containing 1 to 5% of NG. TiO_2 presented large aggregates (**Fig. 1b**) whereas the NG exhibited a smooth and flat surface with some wrinkles (**Fig. 1c**). After hydrothermal reaction, the morphologies of TiO_2/NG nanocomposites with different NG loading were examined and found to differ from pristine TiO_2. Specifically, the particles exhibited rougher surfaces and smaller diameters compared to the pristine TiO_2. It was found that TiO_2/NG5% showed the smallest particles and with the roughest surface among 3 different types of TiO_2/NG nanocomposites (**Fig. 1d – 1f**) while the TiO_2/NG1% showed the biggest particles. This difference in surface area may affect the photocatalytic efficiency as well as laser absorption/desorption behavior.

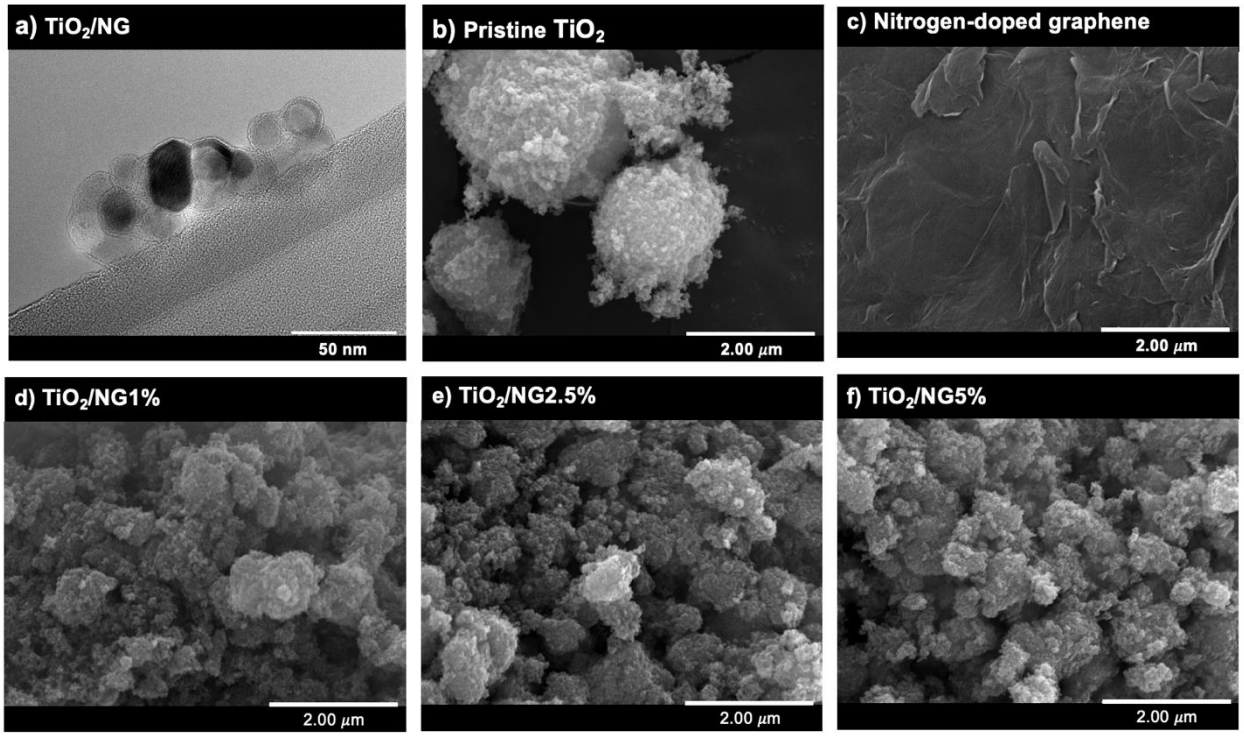

Fig. 1 TEM micrographs of a) TiO_2/ NG nanocomposites with magnification of 250k, and SEM micrographs of b) TiO_2, c) NG, d) TiO_2/NG1%, e) TiO_2/NG2.5%, and f) TiO_2/NG5% nanocomposite with magnification of 20k.

SEM-EDX spectra of TiO_2 and TiO_2/NG nanocomposites are shown in **Fig. 2**. As shown in **Fig. 2a**, the spectra showed peaks of Ti (K, L) and O (K) from the pristine TiO_2, whereas the inset shows mapping of Ti (green) and O (oxygen) from the nanoparticles. After the hydrothermal reaction of TiO_2 with NG (**Fig. 2b**), the high intensity of Ti and O with lower intensity of C and N verifies that NG was successfully coated onto TiO_2 nanoparticles. This is confirmed by the inset illustrating elemental mapping of C and N from NG co-locating with the Ti and O signals.

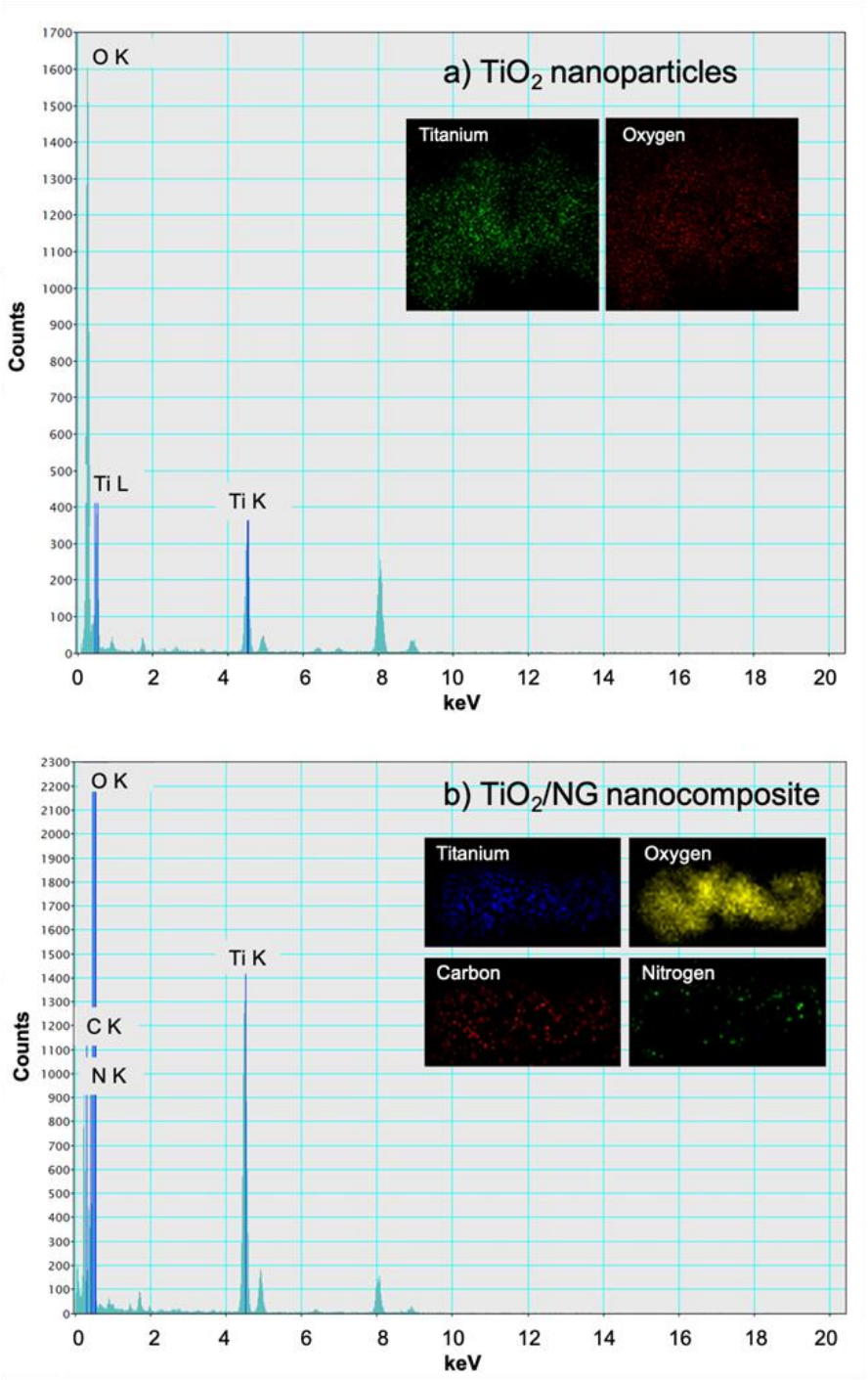

Fig. 2 STEM-EDX analysis and elemental mapping of a) TiO_2 nanoparticles, and b) nano-sized TiO_2/NG nanocomposites. The inset shows mapping of titanium and oxygen from the TiO_2, and carbon and nitrogen from the NG.

XPS was used to investigate the elemental composition and chemical state of materials, as illustrated in **Fig. 3**. As shown in **Fig. 3a**, Ti2p signals of pristine TiO_2 are presented at 455.1 ($2p_{3/2}$), 456.3 (Ti $2p_{3/2}$), and 461.1 eV (Ti $2p_{1/2}$) [49]. The XPS peaks of O1s at 529.9, 532.1, 533.6 and 535.1 eV correspond to different chemical states of O^{2-} in TiO_2 lattice, hydroxyl groups and O^{2-} from water absorption on TiO_2 surface [50]. **Fig. 3b** shows XPS spectra of NG with O1s peaks located at 530.0 (O–C=O), 532.5 (C–OH), and 533.8 (C–O–C) eV [51]. The N1s peak at 401.9 eV is attributed to a graphitic-nitrogen, where a nitrogen atom replaces a carbon atom within the graphene layer [52]. The C1s of pristine NG presents peaks at 281.7 eV, 283.9 eV, which are related to carbon with sp^2 and sp^3 hybridization [53], 284.6 (C–C), 285.5 (C–O) and 287.1 (C=O) eV [51, 54]. The XPS of the TiO_2/NG nanocomposite exhibited peaks shifts from the pristine TiO_2 and NG, as shown in **Fig. 3c**. All Ti2p peaks shifted to higher binding energy caused by electron transfer between O and Ti, consistent with leading to higher amount of Ti^{4+} [55]. The O1s peak shifts are consistent with bond formation of Ti–O_2, C–Ti–O_x (and/or –OR), C–Ti–OH_x (and/or –OR) [56]. In addition, N1s peak located at 399.8 eV shows lower binding energy than NG consistent with the appearance of pyridine-like and pyrrole-like nitrogen [52]. The C1s peak located at 284.6 eV are consistent with the appearance of C–N and/or C–O species, whereas peaks at 286.4 and 288.3 eV can be attributed to C–O bonding in the sample. In summary, the XPS spectra indicated that the chemical state of the TiO_2/NG nanocomposites are modified compared with to the pristine materials.

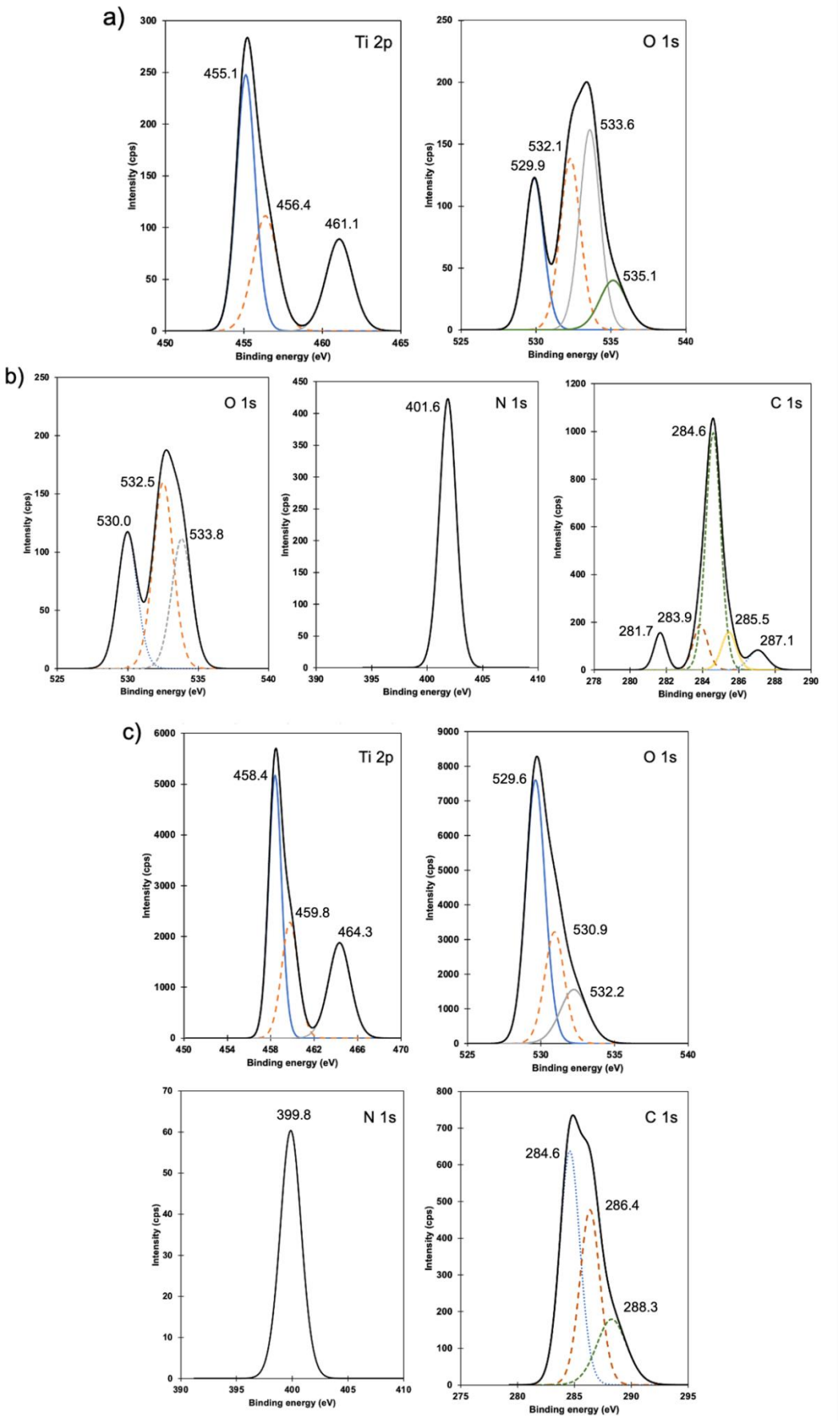
a)
Ti 2p
455.1
456.4
461.1
Intensity (cps)
Binding energy (eV)
O 1s
529.9
532.1
533.6
535.1
b)
O 1s
530.0
532.5
533.8
N 1s
401.6
C 1s
284.6
281.7
283.9
285.5
287.1
c)
Ti 2p
458.4
459.8
464.3
O 1s
529.6
530.9
532.2
N 1s
399.8
C 1s
284.6
286.4
288.3

Fig. 3 XPS spectra of a) TiO_2, b) NG, and c) TiO_2/NG nanocomposite.

3.2 Band gap estimation

The band gap energies of TiO_2/NG nanocomposites were calculated using the Tauc function. As presented in **Fig. 4a**, the band gap energy value of pristine TiO_2 in anatase form is 3.27 eV. The NG concentrations were varied from 1.0% w/w to 15.0% w/w. After mixing NG with TiO_2 and processing using a hydrothermal reaction, the band gaps were altered. Although an alteration was observed upon adding 1.0% w/w NG, the band gap decreased rapidly when NG concentration increased from 2.5% to 5.0%, reaching the lowest band gap energy of 2.69 eV. Further increase in NG concentration to 7.5% resulted in an increase in the band gap energy to 3.41ev followed by a decrease to 3.19 eV at the highest concentration, 15% w/w. Subsequent property measurements were carried out on the TiO_2/NG nanocomposite containing 2.5%NG, which exhibits the lowest band gap as 2.69 eV.

Using UV-visible spectroscopy, the spectra in **Fig. 4b** show the absorbance of the pristine TiO_2 and TiO_2/NG nanocomposites for NG concentrations from 1 to 15% w/w. The spectra indicated that adding of NG altered the absorbance of TiO_2, which indicates a change in the photocatalytic reaction efficiency. An optimum content of NG at 2.5% w/w was selected for further experiments because this TiO_2/NG nanocomposite exhibited the lowest band gap value.

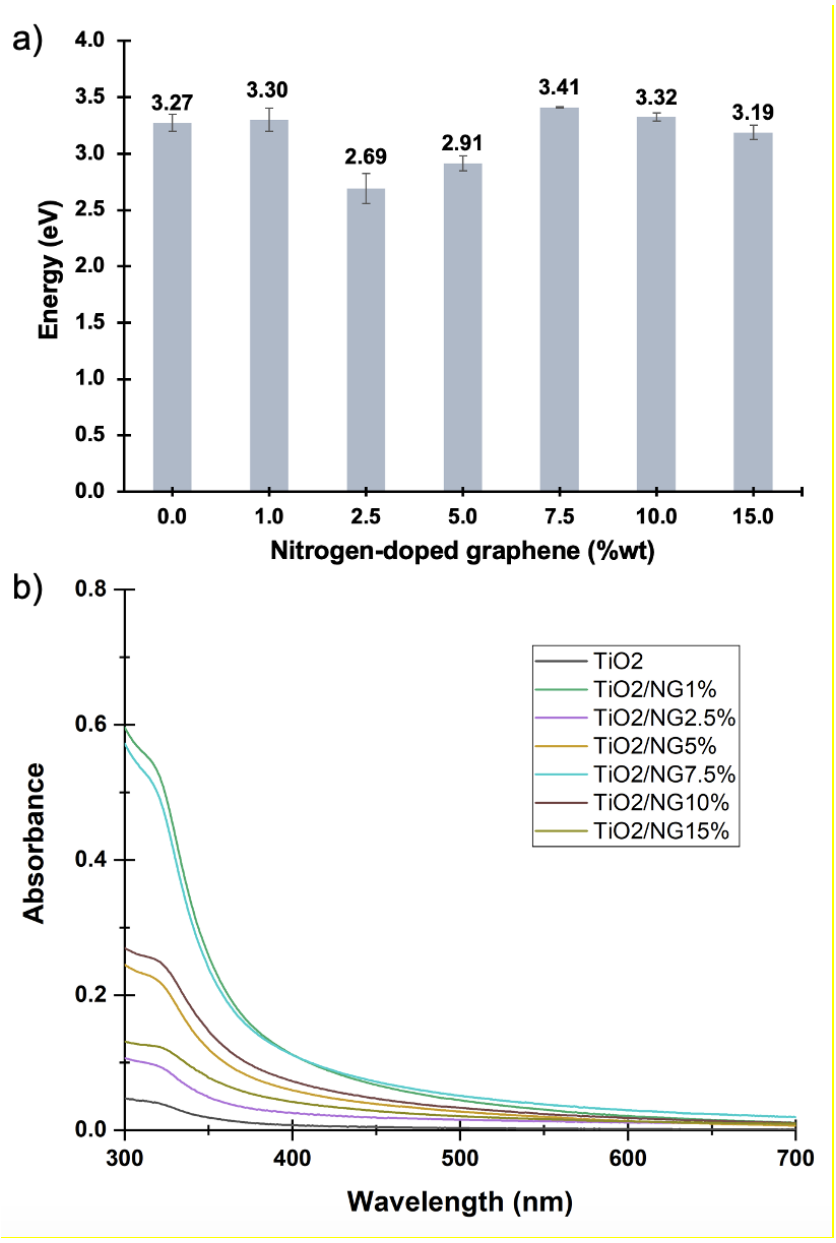

Fig. **4** a) Estimated band gap energy of the TiO_2/NG nanocomposites as a function of NG loading using Tauc function (n=3), and b) UV-visible spectra of TiO_2 and TiO_2/NG nanocomposites with different NG contents.

3.3 Chitosan films with TiO_2/NG

As displayed in **Fig. 5**, the solvent used to spin-coat chitosan and chitosan with TiO_2/NG affected film quality. The spin-coated CH using 1% acetic acid (**Fig. 5a**) displayed non-homogeneous films with large comets radiating outward from the center of the silicon wafer, which was possibly caused by low viscosity of the CH/solvent solution. Since IPA is known to disperse NG [57], IPA was mixed with acidic acid (1% acetic acid with 50% IPA). It was found that films prepared with neat CH and chitosan with TiO_2/NG exhibited thicknesses of 209.1 ± 17.2 nm (**Fig. 5b**) and 302.5 ± 9.4 nm (**Fig. 5c**), respectively. These high-quality films exhibited fewer defects and have a uniform color across the 1 cm x 1 cm silicon substrate. The change in color near the edges of the substrate were caused by a change in film thickness associated with the spin coating process itself. The better film formation using the acetic acid/IPA solvent mixture, which is a non-toxic cosolvent[58-60], was due to the higher viscosity of CH solution caused by IPA addition. The grayish color in **Fig. 5a** indicates a thinner film, compared with the blueish color in **Fig. 5b and 5c**.

Film thickness of chitosan was measured as a function of chitosan concentration. The thickness of CH films spin cast from acetic acid increased from 17nm to 56nm but exhibited a large standard deviation consistent with poor film quality as plotted in **Fig. 5d**. On the other hand, CH films spin cast from a mixture of acetic acid and IPA increased from 16nm to 292nm with relatively low standard deviation (**Fig. 5e**) consistent with the homogeneity of the spin-coated films. Accordingly, a CH concentration of 1.5% w/w spin cast from a mixture of acetic acid and IPA with a nominal thickness of 200nm was used to prepare chitosan films with TiO_2/NG for further experiments.

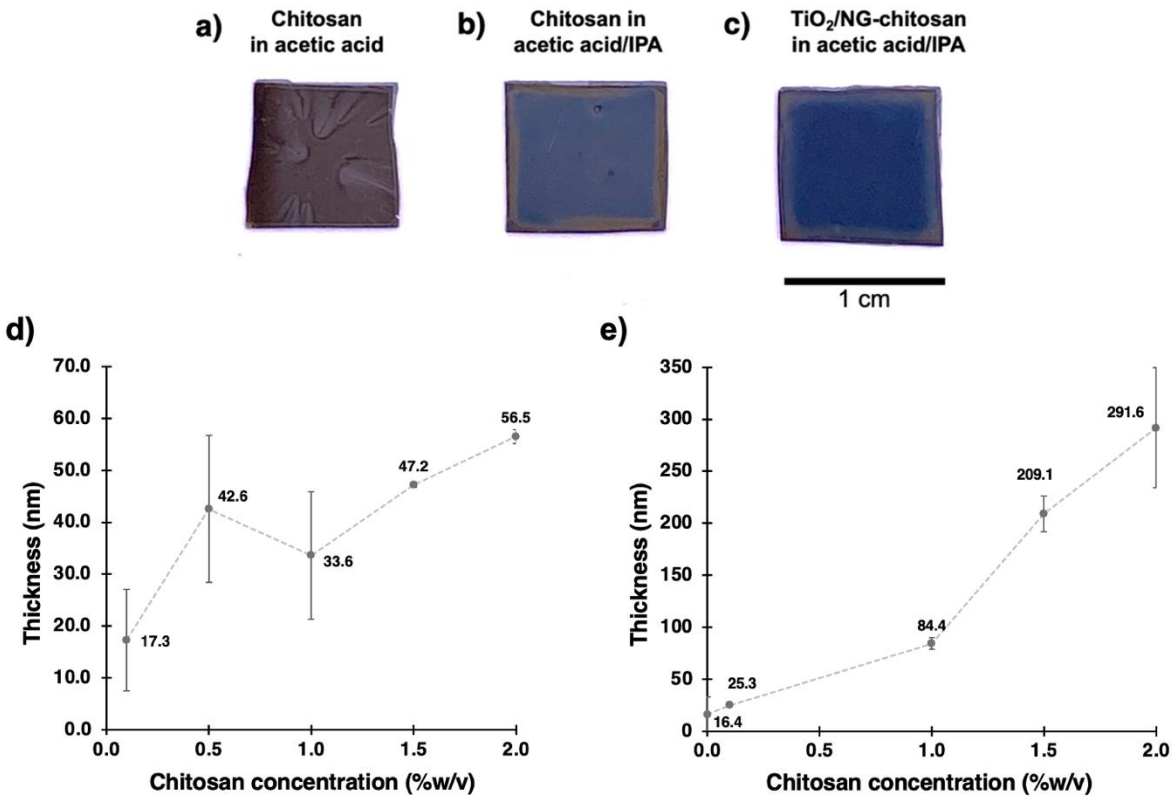

Fig. 5 Photographs of spin-coated silicon wafer of: a) chitosan dissolved in acetic acid, b) chitosan dissolved in acetic acid/isopropanol, and c) chitosan with TiO_2/NG nanocomposite dispersed in acetic acid/isopropanol, and d) thickness of spin-coated chitosan thin film dissolved in acetic acid, e) thickness of spin-coated chitosan thin film dissolved in acetic acid/isopropanol using 5000 rpm (n=3).

3.4 Photocatalytic activity of chitosan films with TiO_2/NG

The photocatalytic activity of the TiO_2/NG-CH films was evaluated under the visible light irradiation. The nanocomposite films were exposed to ciprofloxacin solution to investigate the degradation of pristine chitosan films as well as those containing particles, namely TiO_2-CH, NG-CH, and TiO_2/NG-CH. Because as-cast films are smooth, the surface roughness determined from

AFM can be used as an indication of the extent of degradation of films upon exposure. As displayed in **Fig. 6a**, at time 0 min, all as-prepared films were relatively smooth with a surface roughness from 0.3 nm to 0.6 nm. The addition of nanomaterials increased the roughness (Ra) of the films. Averaged across 10 x 10 micron image, the Ra for the as cast films increases from 0.3, 0.5, 0.5, and 0.6 nm, respectively. The higher roughness value of TiO_2/NG-CH compared to TiO_2-CH and NG-CH might be due to the higher concentration of TiO_2/NG nanoparticles dispersed in the chitosan film after filtration since the size of TiO_2/NG nanoparticles was smaller than the pristine NG and TiO_2 nanoparticles and exhibited better dispersity in CH solution.

After 30 min of exposure with visible light, the surface roughness of all films increased, including the pure CH film (10x). This might be due to the degradation or swelling behavior of CH since pKa of ciprofloxacin is 6.09 [61] leading to protonation of CH. In all cases though the films containing chitosan were rougher than the chitosan control film at 30 min and 60 min. After 30 min of ciprofloxacin exposure, the surface roughness of all films increased dramatically, particularly the films containing NG (NG-CH and TiO_2/NG-CH). The high regions are bright whereas the low regions are dark (see color scale to right of height image). After 30 min of exposure, the roughness of the NG-CH and TiO_2/NG-CH films are similar (13.0 nm vs 12.4 nm) as shown in **Fig. 6**. Interestingly, at 60 min of exposure, the roughness of all film decreased, except NG-CH with no significant difference. This result suggested that CH (carrier polymer) was degraded and the silicon wafer, denoted by the low (dark) areas, was directly exposed to the ciprofloxacin solution. Thus, degradation of the "high" regions occurs whereas the lower regions remain the same. Thus, 60 min of ciprofloxacin exposure was selected to study the photocatalytic efficiency of chitosan nanocomposite films.

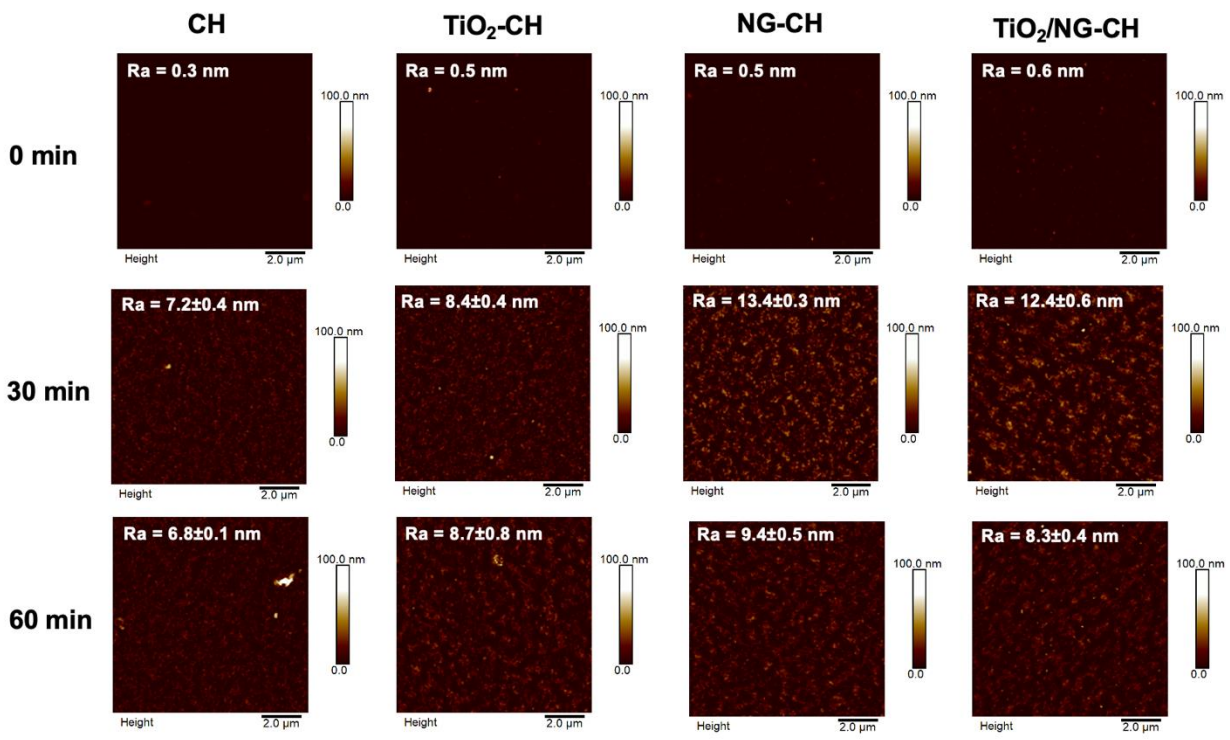

Fig. 6 AFM images and surface roughness of thin films: a) CH, b) CH with TiO_2, c) CH with NG, and d) CH with TiO_2/NG nanocomposite after exposed to 50 µg/mL Ciprofloxacin at different time intervals (n=3).

Photocatalytic mechanism is described next. Based on a conventional photocatalyst, TiO_2, photons with higher energy than the band gap of the photocatalyst produces •OH by oxidizing -OH/H_2O or ciprofloxacin, and degrades ciprofloxacin to its intermediates and final product, respectively [62, 63]. Ciprofloxacin is a zwitterionic compound. However, it was observed that ciprofloxacin dissolved in DI water at a concentration of 50 µg/mL resulted in a pH range of approximately pH = 8.15 - 8.33 indicating a basic solution. In this environment, it was noted that the CH polymeric carrier was unable to dissolve in the ciprofloxacin solution. This confirmed that

the degradation of ciprofloxacin and CH can be attributed to the embedded TiO_2-containing photocatalysts.

3.5 Photocatalytic efficiency of chitosan films with TiO_2 and NG

To investigate the photocatalytic activity of chitosan films with TiO_2 and NG, the photocatalytic degradation of ciprofloxacin was studied. Films of CH, TiO_2-CH, NG-CH, and TiO_2/NG-CH on silicon wafers (1.0×1.0 cm^2) were immersed in 50 μg/mL ciprofloxacin solution without adding H_2O_2, and exposed to visible light for 60 min. The results show that TiO_2/NG-CH films exhibit significantly higher photodegradation efficiency (%) than TiO_2-CH (4.44±0.38%) and NG-CH (3.60±1.06%), as shown in **Fig. 7a**. We attribute this higher efficiency to the reduced band gap of the TiO_2/NG nanocomposites resulting in enhanced absorption of light in the visible range. Interestingly, although it did not exhibit the lowest calculated band gap, the highest photodegradation efficiency was observed for TiO_2/NG5%-CH film (34.16±0.06%). This result might be possibly related to the adsorption of ciprofloxacin on the surface of TiO_2/NG5%-CH films [64], attributed to an attractive interaction between ciprofloxacin and the TiO_2/NG nanocomposite. This attraction likely results from strong binding between the aromatic rings of ciprofloxacin with the graphitic structure of NG via π-π interaction, as well as hydrogen bonding between ciprofloxacin and NG in the nanocomposites. Significantly, the TiO_2/NG5% nanocomposite had higher surface area due to smaller particles in comparison to TiO_2/NG1% (26.3±0.4% in efficiency), and TiO_2/NG2.5% (28.9±0.3% in efficiency) with the lowest calculated band gap. The absorbance intensity indicates the concentration of ciprofloxacin as shown in **Fig. 7b**. The absorbance of ciprofloxacin in CH films with TiO_2/NG was lower than CH films with TiO_2 and NG alone. The lowest absorbance of degraded ciprofloxacin using TiO_2/NG

nanocomposite-CH thin films were TiO_2/NG5%, TiO_2/NG2.5%, and TiO_2/NG1%, respectively. Thus, TiO_2NG5%-CH film was the most suitable nanocomposite-containing biopolymeric film for ciprofloxacin degradation application.

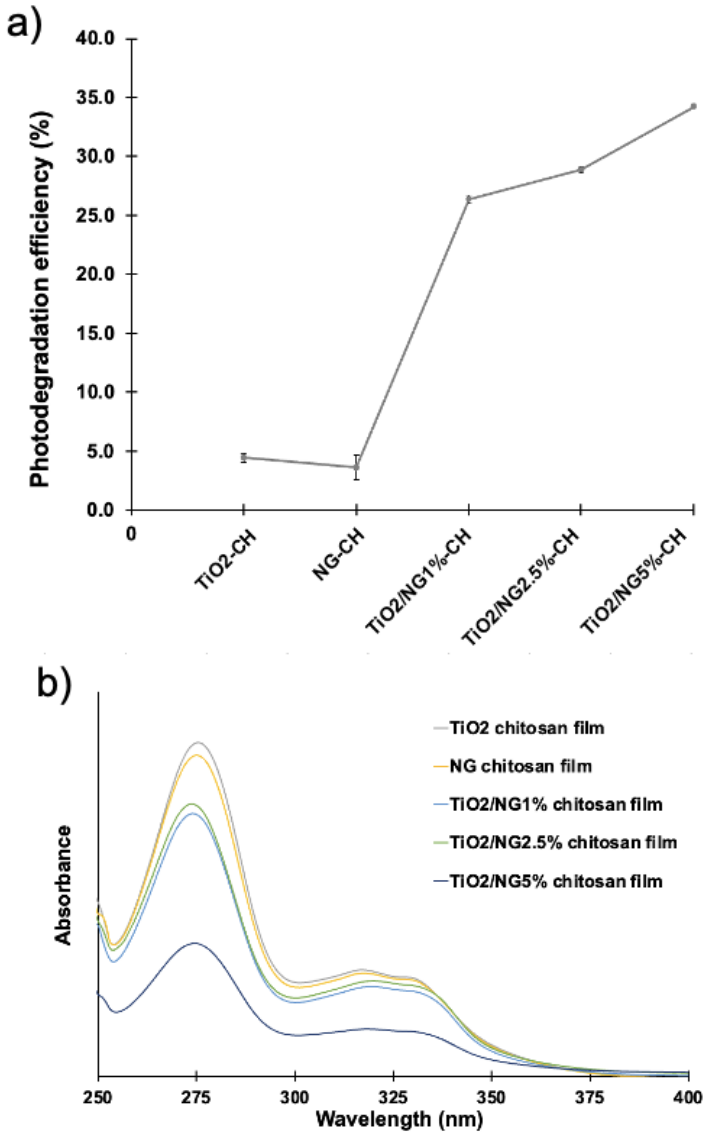

Fig. 7 a) Photodegradation efficiency (%) of CH-based thin films towards ciprofloxacin under 60 min of irradiation (n=3), and b) ciprofloxacin spectra after 60 min of irradiation.

3.6 chitosan films with TiO_2 and NG as a solid matrix for LDI-MS

As a second application, **Fig. 8** displays LDI-MS spectra of chitosan films with TiO_2 and NG as a solid matrix for LDI-MS to identify peptides. As displayed in **Fig. 8a**, the uncoated wafer with conventional matrix showed the ability to determine angiotensin II, angiotensin I, substance P, and bombesin but exhibited relatively low S/N ratio (signal-to-noise ratio) and high background noise. In contrast, chitosan films with TiO_2/NG on silicon were able to identify peptide biomarkers including angiotensin II, angiotensin I, substance P, ACTH (1-17), ACTH (18-39), and somatostatin 28 (**Fig. 8b**) with high signal/noise ration. The improved performance of the TiO_2/NG-CH nanocomposite might be due to ability of the enrichment of peptides on the TiO_2, adsorption properties of NG and laser efficiency due to the nano-sized particles. These biomarkers indicate the physiological state of the human body. For instance, angiotensin I, angiotensin II, and ACTH are related to arterial pressure and hydro-electrolyte balance [65], cell growth regulation [66], and post-stroke depression [67], respectively. Moreover, the silicon wafer with the coated exhibited high signal intensity at low m/z (mass-to-charge ratio) with high S/N ratio. These results demonstrate the promising potential of TiO_2/NG-CH films as an alternative substrate for LDI-MS in peptide biomarker identification to diagnose diseases.

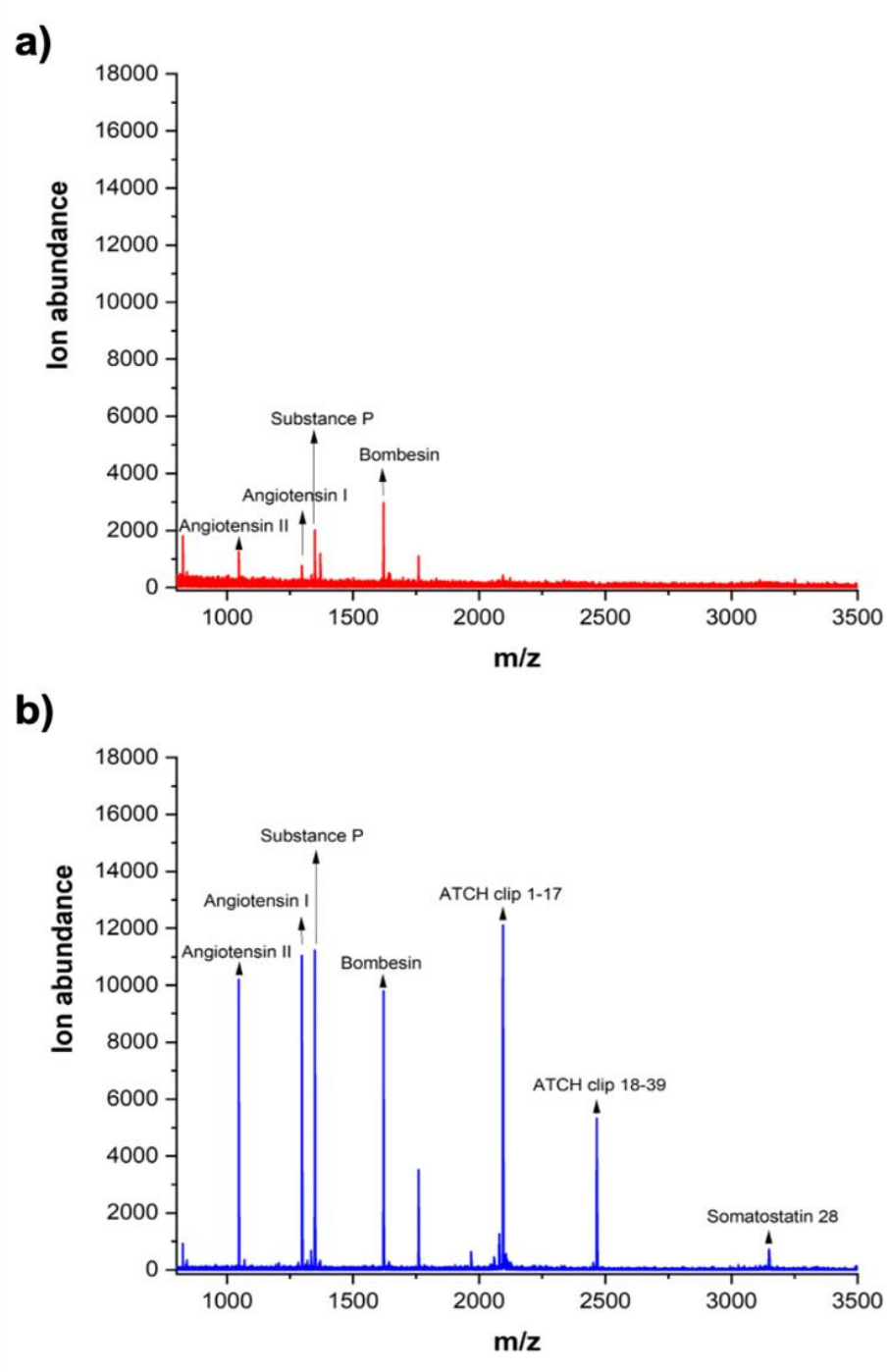

Fig. 8 LDI-MS spectra of standard peptides measured using a) uncoated silicon wafer, and b) TiO_2/NG nanocomposite-CH coated silicon wafer.

Conclusions

Nano-sized TiO_2/NG were synthesized via hydrothermal reaction to enhance photocatalysis, UV-Visible absorption and laser absorption properties. The band gap of nanocomposite was lower than pristine TiO_2, decreasing from 3.37 eV to 2.69 eV, indicating the higher light absorption capacity of TiO_2/NG. These nanoparticles were embedded in chitosan by spin coating on a silicon wafer to create nanocomposite-biopolymer films and shown to degrade ciprofloxacin without adding H_2O_2. These nanocomposite films exhibited higher photocatalytic activity towards ciprofloxacin compared to TiO_2-chitosan and NG-chitosan films. Furthermore, the nanocomposite film was successfully tested as a sensitive LDI-MS solid matrix that can be used to detect peptide biomarkers for disease diagnosis. In summary, this novel film might be a promising material for pollutant degradation and biomarkers detection in the future.

Acknowledgements

This research was supported by the Second Century Fund (C2F), Chulalongkorn University, Thailand. R.J.C. and TS were supported by the National Science Foundation Partnerships for International Research and Education Program (NSF-PIRE), Grant #1545884. This work was additionally supported by the POLYMERS-DMR-1905912 (R.J.C.) and MRSEC-DMR-1720530 (R.J.C.) programs. This work was carried out in part at the Singh Center for Nanotechnology, which is supported by the NSF National Nanotechnology Coordinated Infrastructure Program under grant NNCI-2025608.

References

[1] Qiu, Y., J. Cheng, H. Guo, Z. Zhang, W. Yang, and K. Cen. Mild hydrothermal treatment on microalgal biomass in batch reactors for lipids hydrolysis and solvent-free extraction to produce biodiesel, Energy. 189 (2019) 116308. https://doi.org/10.1016/j.energy.2019.116308.

[2] Sinhamahapatra, A., N. Sutradhar, B. Roy, A. Tarafdar, H.C. Bajaj, and A.B. Panda. Mesoporous zirconium phosphate catalyzed reactions: Synthesis of industrially important chemicals in solvent-free conditions, Appl. Catal. 385 (2010) 22-30. https://doi.org/10.1016/j.apcata.2010.06.016.

[3] Jabbar, Z.H., B.H. Graimed, S.H. Ammar, D.A. Sabit, A.A. Najim, A.Y. Radeef, and A.G. Taher. The latest progress in the design and application of semiconductor photocatalysis systems for degradation of environmental pollutants in wastewater: Mechanism insight and theoretical calculations, Materials Science in Semiconductor Processing. 173 (2024) 108153. https://doi.org/10.1016/j.mssp.2024.108153.

[4] Vento, F., A. Nicosia, L. Mezzina, G. Raciti, A. Gulino, M. Condorelli, L. D'Urso, G. De Guidi, and P. Mineo. Photocatalytic Activity of TiO2-Containing Nanocomposites versus the Chemical Nature of the Polymeric Matrices: A Comparison, Adv. Mater. Technol. 8 (2023) 2300391. https://doi.org/10.1002/admt.202300391.

[5] Rangarajan, G., G. Kannappan Panchamoorthy, V. Nagarajan, A. Krishnan, and M. R. Present applications of titanium dioxide for the photocatalytic removal of pollutants from water: A review, J. Environ. Manage. 270 (2020). https://doi.org/10.1016/j.jenvman.2020.110906.

[6] Guo, Q., C. Zhou, Z. Ma, and X. Yang. Fundamentals of TiO2 Photocatalysis: Concepts, Mechanisms, and Challenges, Adv. Mater. 31 (2019) 1901997. https://doi.org/10.1002/adma.201901997.

[7] Piler, K., C. Bahrim, S. Twagirayezu, and T.J. Benson, Chapter Two - Lattice disorders of TiO2 and their significance in the photocatalytic conversion of CO2, in Adv. Catal, C. Song, Editor. 2020, Academic Press.109-233.https://doi.org/10.1016/bs.acat.2020.09.001.

[8] Gao, M., L. Zhu, C.K. Peh, and G.W. Ho. Solar absorber material and system designs for photothermal water vaporization towards clean water and energy production, Energy Environ. Sci. 12 (2019) 841-864. https://doi.org/10.1039/C8EE01146J.

[9] Suriani, A.B., Muqoyyanah, A. Mohamed, M.H. Mamat, M.H.D. Othman, M.K. Ahmad, H.P.S. Abdul Khalil, P. Marwoto, and M.D. Birowosuto. Titanium dioxide/agglomerated-free reduced graphene oxide hybrid photoanode film for dye-sensitized solar cells photovoltaic performance improvement, Nano-Struct. Nano-Objects. 18 (2019) 100314. https://doi.org/10.1016/j.nanoso.2019.100314.

[10] Passornraprasit, N., T. Siripongpreda, S. Ninlapruk, N. Rodthongkum, and P. Potiyaraj. γ-Irradiation crosslinking of graphene oxide/cellulose nanofiber/poly (acrylic acid) hydrogel as a urea sensing patch, Int. J. Biol. Macromol. 213 (2022) 1037-1046. https://doi.org/10.1016/j.ijbiomac.2022.06.053.

[11] Li, S.-M., et al. N-doped structures and surface functional groups of reduced graphene oxide and their effect on the electrochemical performance of supercapacitor with organic

electrolyte, J. Power Sources. 278 (2015) 218-229. https://doi.org/10.1016/j.jpowsour.2014.12.025.
[12] Tian, G., L. Liu, Q. Meng, and B. Cao. Facile synthesis of laminated graphene for advanced supercapacitor electrode material via simultaneous reduction and N-doping, J. Power Sources. 274 (2015) 851-861. https://doi.org/10.1016/j.jpowsour.2014.10.171.
[13] Pan, Z., et al. Anchoring FeRu Bimetallic Nanoparticles on N-Doped Graphene Nanosheets for Efficient Overall Water Splitting, Energy & Fuels. 38 (2024) 3303-3311. 10.1021/acs.energyfuels.3c04249.
[14] Putri, L.K., W.-J. Ong, W.S. Chang, and S.-P. Chai. Heteroatom doped graphene in photocatalysis: A review, Appl. Surf. Sci. 358 (2015) 2-14. https://doi.org/10.1016/j.apsusc.2015.08.177.
[15] Luque-Centeno, J.M., M.V. Martínez-Huerta, D. Sebastián, S. Pérez-Rodríguez, and M.J. Lázaro. Titanium Dioxide/N-Doped Graphene Composites as Non-Noble Bifunctional Oxygen Electrocatalysts, Ind. amp; Eng. Chem. 60 (2021) 18817-18830. https://doi.org/10.1021/acs.iecr.1c02896.
[16] Cammarata, A., M. Kaintz, and T. Polcar. Engineering width and directness of the band gap in diamond-based materials: An ab initio investigation towards electron-structure features control, Diam. Relat. Mater. 128 (2022) 109237. https://doi.org/10.1016/j.diamond.2022.109237.
[17] Hight-Huf, N., et al. Polarization-Driven Asymmetric Electronic Response of Monolayer Graphene to Polymer Zwitterions Probed from Both Sides, Appl. Mater. Interfaces. 13 (2021) 47945-47953. https://doi.org/10.1021/acsami.1c13505.
[18] Bie, C., H. Yu, B. Cheng, W. Ho, J. Fan, and J. Yu. Design, Fabrication, and Mechanism of Nitrogen-Doped Graphene-Based Photocatalyst, Adv. Mater. 33 (2021) 2003521. https://doi.org/10.1002/adma.202003521.
[19] Hu, W.-Y., et al. Facilitating Hot Electron Injection from Graphene to Semiconductor by Rectifying Contact for Vis–NIR-Driven H2O2 Production, Small. 18 (2022) 2200885. https://doi.org/10.1002/smll.202200885.
[20] Shen, T., D. Lang, F. Cheng, and Q. Xiang. Ternary Reduced Graphene Oxide/g-C3N4/Ag-AgCl Nanocomposites for Controlled Visible-Light Photocatalytic Selectivity, ChemistrySelect. 1 (2016) 1006-1015. https://doi.org/10.1002/slct.201600041.
[21] Kumar, P., A. Kumar, C. Joshi, R. Boukherroub, and S.L. Jain, Graphene–Semiconductor Hybrid Photocatalysts and Their Application in Solar Fuel Production, in Advanced 2D Materials. 2016.353-386.https://doi.org/10.1002/9781119242635.ch9.
[22] Baragau, I.-A., et al. Outstanding visible light photocatalysis using nano-TiO2 hybrids with nitrogen-doped carbon quantum dots and/or reduced graphene oxide, J. Mater. Chem. A. 11 (2023) 9791-9806. https://doi.org/10.1039/D2TA09586F.
[23] Hou, J., H. Cheng, O. Takeda, and H. Zhu. Three-Dimensional Bimetal-Graphene-Semiconductor Coaxial Nanowire Arrays to Harness Charge Flow for the Photochemical Reduction of Carbon Dioxide, Angew. Chem., Int. Ed. Engl. 54 (2015) 8480-8484. https://doi.org/10.1002/anie.201502319.
[24] Padmanabhan, N.T., N. Thomas, J. Louis, D.T. Mathew, P. Ganguly, H. John, and S.C. Pillai. Graphene coupled TiO2 photocatalysts for environmental applications: A review, Chemosphere. 271 (2021) 129506. https://doi.org/10.1016/j.chemosphere.2020.129506.

[25] González-Torres, J.C., E. Poulain, V. Domínguez-Soria, R. García-Cruz, and O. Olvera-Neria. C-, N-, S-, and F-Doped Anatase TiO₂ (101) with Oxygen Vacancies: Photocatalysts Active in the Visible Region, Int. J. Photoenergy. 2018 (2018) 7506151. https://doi.org/10.1155/2018/7506151.

[26] Liu, C., et al. Hydrothermal synthesis of N-doped TiO2 nanowires and N-doped graphene heterostructures with enhanced photocatalytic properties, J. Alloys Compd. 656 (2016) 24-32. https://doi.org/10.1016/j.jallcom.2015.09.211.

[27] Ning, D., J. Zhang, A. Murali, Y. Lan, C. Chen, S. Yang, W. Zhang, and J. Li. Advancements in organic pollutant remediation: The role of nitrogen-doped rGO-CeO2 in photocatalytic efficiency enhancement, Colloids and Surfaces A: Physicochemical and Engineering Aspects. 685 (2024) 133282. https://doi.org/10.1016/j.colsurfa.2024.133282.

[28] Zhou, Y., D. Jiang, Z. Wang, L. Yi, J. Sun, D. Liu, X. Yu, and Y. Chen. Bandgap engineering of carbon nitride by formic acid assisted thermal treatment for photocatalytic degradation of tetracycline hydrochloride, Chemical Engineering Journal. 485 (2024) 149830. https://doi.org/10.1016/j.cej.2024.149830.

[29] Aranaz, I., A.R. Alcántara, M.C. Civera, C. Arias, B. Elorza, A. Heras Caballero, and N. Acosta Chitosan: An Overview of Its Properties and Applications. Polymers, 2021. 13, DOI: https://doi.org/10.3390/polym13193256.

[30] Xu, N., S. Gao, C. Xu, Y. Fang, L. Xu, and W. Zhang. Carbon quantum dots derived from waste acorn cups and its application as an ultraviolet absorbent for polyvinyl alcohol film, Appl. Surf. Sci. 556 (2021) 149774. https://doi.org/10.1016/j.apsusc.2021.149774.

[31] Nalam, P.C., H.-S. Lee, N. Bhatt, R.W. Carpick, D.M. Eckmann, and R.J. Composto. Nanomechanics of pH-Responsive, Drug-Loaded, Bilayered Polymer Grafts, ACS Appl. Mater. Interfaces. 9 (2017) 12936-12948. https://doi.org/10.1021/acsami.6b14116.

[32] Zhang, Y., F. Liu, L. Zhong, Z. Dong, C. Chen, and Z. Xu. Reusable and environmentally friendly cellulose nanofiber/titanium dioxide/chitosan aerogel photocatalyst for efficient degradation of tetracycline, Appl. Surf. Sci. 641 (2023) 158425. https://doi.org/10.1016/j.apsusc.2023.158425.

[33] Pagaduan, J.N., N. Hight-Huf, A. Datar, Y. Nagar, M. Barnes, D. Naveh, A. Ramasubramaniam, R. Katsumata, and T. Emrick. Electronic Tuning of Monolayer Graphene with Polymeric "Zwitterists", ACS Nano. 15 (2021) 2762-2770. https://doi.org/10.1021/acsnano.0c08624.

[34] Salman, M.S., et al. Chitosan-coated cotton fiber composite for efficient toxic dye encapsulation from aqueous media, Appl. Surf. Sci. 622 (2023) 157008. https://doi.org/10.1016/j.apsusc.2023.157008.

[35] Kim, M.-J., J.-M. Park, T.G. Yun, J.-Y. Noh, M.-J. Kang, and J.-C. Pyun. A TiO2 nanowire photocatalyst for dual-ion production in laser desorption/ionization (LDI) mass spectrometry, ChemComm. 56 (2020) 4420-4423. https://doi.org/10.1039/D0CC00866D.

[36] Zhang, Y., B. Zhou, Q. Li, M. Jin, and Y. Bai. Nanomaterial Assisted Exosome Analysis Using Mass Spectrometry, Chemical Research in Chinese Universities. (2024). 10.1007/s40242-024-4004-x.

[37] Zhen, Z. and H. Zhu, 1 - Structure and Properties of Graphene, in Graphene, H. Zhu, et al., Editors. 2018, Academic Press.1-12.https://doi.org/10.1016/B978-0-12-812651-6.00001-X.

[38] Shi, C.Y. and C.H. Deng. Recent advances in inorganic materials for LDI-MS analysis of small molecules, Analyst. 141 (2016) 2816-2826. https://doi.org/10.1039/C6AN00220J.
[39] Min, Q., X. Zhang, X. Chen, S. Li, and J.-J. Zhu. N-Doped Graphene: An Alternative Carbon-Based Matrix for Highly Efficient Detection of Small Molecules by Negative Ion MALDI-TOF MS, Anal. Chem. 86 (2014) 9122-9130. https://doi.org/10.1021/ac501943n.
[40] M, A. and R. N.K. Graphene–dye hybrid optical sensors, Nano-Struct. Nano-Objects. 17 (2019) 194-217. https://doi.org/10.1016/j.nanoso.2019.01.003.
[41] Picó, Y. and D. Barceló. Mass Spectrometry in Wastewater-Based Epidemiology for the Determination of Small and Large Molecules as Biomarkers of Exposure: Toward a Global View of Environment and Human Health under the COVID-19 Outbreak, ACS Omega. 6 (2021) 30865-30872. https://doi.org/10.1021/acsomega.1c04362.
[42] Schwab, M., Peptide Biomarkers, in Encyclopedia of Cancer. 2011, Springer Berlin Heidelberg. pp. 2809-2810.
[43] Han, T., H. Cong, T. Yu, and Y. Shen. Application of peptide biomarkers in life analysis based on liquid chromatography–mass spectrometry technology, BioFactors. 48 (2022) 725 - 743. https://doi.org/10.1002/biof.1875.
[44] Maguire, S.M., J.B. McClimon, A.C. Zhang, A.W. Keller, C.R. Bilchak, K. Ohno, R.W. Carpick, and R.J. Composto. Nanoscale Structure–Property Relations in Self-Regulated Polymer-Grafted Nanoparticle Composite Structures, ACS Appl. Mater. Interfaces. 15 (2023) 10974-10985. https://doi.org/10.1021/acsami.2c15786.
[45] Makuła, P., M. Pacia, and W. Macyk. How To Correctly Determine the Band Gap Energy of Modified Semiconductor Photocatalysts Based on UV–Vis Spectra, J. Phys. Chem. Lett. 9 (2018) 6814-6817. https://doi.org/10.1021/acs.jpclett.8b02892.
[46] Kolář, M., H. Měšt'ánková, J. Jirkovský, M. Heyrovský, and J. Šubrt. Some Aspects of Physico-Chemical Properties of TiO2 Nanocolloids with Respect to Their Age, Size, and Structure, Langmuir. 22 (2006) 598-604. https://doi.org/10.1021/la058016w.
[47] Karimi, L., S. Zohoori, and M.E. Yazdanshenas. Photocatalytic degradation of azo dyes in aqueous solutions under UV irradiation using nano-strontium titanate as the nanophotocatalyst, J. Saudi Chem. Soc. 18 (2014) 581-588. https://doi.org/10.1016/j.jscs.2011.11.010.
[48] Hidayat, R., G. Fadillah, and S. Wahyuningsih. A control of TiO2 nanostructures by hydrothermal condition and their application: a short review, IOP Conf. Ser.: Mater. Sci. Eng. 578 (2019) 012031. https://doi.org/10.1088/1757-899X/578/1/012031.
[49] Guillot, J., A. Jouaiti, L. Imhoff, B. Domenichini, O. Heintz, S. Zerkout, A. Mosser, and S. Bourgeois. Nitrogen plasma pressure influence on the composition of TiNxOy sputtered films, Surf. Interface Anal. 33 (2002) 577-582. https://doi.org/10.1002/sia.1423.
[50] Fang, Y., W. Huang, S. Yang, X. Zhou, C. Ge, Q. Gao, Y. Fang, and S. Zhang. Facile synthesis of anatase/rutile TiO2/g-C3N4 multi-heterostructure for efficient photocatalytic overall water splitting, Int. J. Hydrogen Energy. 45 (2020) 17378-17387. https://doi.org/10.1016/j.ijhydene.2020.04.214.
[51] Al-Gaashani, R., A. Najjar, Y. Zakaria, S. Mansour, and M.A. Atieh. XPS and structural studies of high quality graphene oxide and reduced graphene oxide prepared by different chemical oxidation methods, Ceram. Int. 45 (2019) 14439-14448. https://doi.org/10.1016/j.ceramint.2019.04.165.

[52] Sheng, Z.-H., L. Shao, J.-J. Chen, W.-J. Bao, F.-B. Wang, and X.-H. Xia. Catalyst-Free Synthesis of Nitrogen-Doped Graphene via Thermal Annealing Graphite Oxide with Melamine and Its Excellent Electrocatalysis, ACS Nano. 5 (2011) 4350-4358. https://doi.org/10.1021/nn103584t.

[53] Drewniak, S., R. Muzyka, A. Stolarczyk, T. Pustelny, M. Kotyczka-Morańska, and M. Setkiewicz Studies of Reduced Graphene Oxide and Graphite Oxide in the Aspect of Their Possible Application in Gas Sensors. Sensors, 2016. 16, DOI: https://doi.org/10.3390/s16010103.

[54] Johra, F.T., J.-W. Lee, and W.-G. Jung. Facile and safe graphene preparation on solution based platform, J. Ind. Eng. Chem. 20 (2014) 2883-2887. https://doi.org/10.1016/j.jiec.2013.11.022.

[55] Jackman, M.J., A.G. Thomas, and C. Muryn. Photoelectron Spectroscopy Study of Stoichiometric and Reduced Anatase TiO2(101) Surfaces: The Effect of Subsurface Defects on Water Adsorption at Near-Ambient Pressures, J. Phys. Chem. C. 119 (2015) 13682-13690. https://doi.org/10.1021/acs.jpcc.5b02732.

[56] Natu, V., M. Benchakar, C. Canaff, A. Habrioux, S. Célérier, and M.W. Barsoum. A critical analysis of the X-ray photoelectron spectra of Ti3C2Tz MXenes, Matter. 4 (2021) 1224-1251. https://doi.org/10.1016/j.matt.2021.01.015.

[57] Pace, G., et al. Nitrogen-doped graphene based triboelectric nanogenerators, Nano Energy. 87 (2021) 106173. https://doi.org/10.1016/j.nanoen.2021.106173.

[58] Liu, X., S. Veldhuis, R. Mathews, and I. Zhitomirsky. Dip coating of poly(ethyl methacrylate) and composites from solutions in isopropanol-water co-solvent, Colloids Surf. A: Physicochem. Eng. 631 (2021) 127703. https://doi.org/10.1016/j.colsurfa.2021.127703.

[59] Yildiz, B.C. and A. Kayan. Non-Toxic and Environmentally Friendly Titanium Complexes and Their Effects on Ɛ-Caprolactone Polymerization, Catal. Surv. from Asia. 24 (2020) 313-324. https://doi.org/10.1007/s10563-020-09307-3.

[60] He, Q., H. Zhang, S. Han, Y. Xing, Y. Li, X. Zhang, and R. Wang. Improvement of green antisolvent-isopropanol and additive-thiourea on carbon based CsPbIBr2 perovskite solar cells, Mater. Sci. Semicond. Process. 150 (2022) 106940. https://doi.org/10.1016/j.mssp.2022.106940.

[61] Sharma, P.C., A. Jain, S. Jain, R. Pahwa, and M.S. Yar. Ciprofloxacin: review on developments in synthetic, analytical, and medicinal aspects, J. Enzyme Inhib. Med. Chem. 25 (2010) 577-589. https://doi.org/10.3109/14756360903373350.

[62] Shehu Imam, S., R. Adnan, and N.H. Mohd Kaus. Photocatalytic degradation of ciprofloxacin in aqueous media: a short review, Toxicol. Environ. Chem. 100 (2018) 518-539. https://doi.org/10.1080/02772248.2018.1545128.

[63] Jiménez-Salcedo, M., M. Monge, and M.T. Tena. Study of intermediate by-products and mechanism of the photocatalytic degradation of ciprofloxacin in water using graphitized carbon nitride nanosheets, Chemosphere. 247 (2020) 125910. https://doi.org/10.1016/j.chemosphere.2020.125910.

[64] Yang, Y., L. Xu, H. Wang, W. Wang, and L. Zhang. TiO2/graphene porous composite and its photocatalytic degradation of methylene blue, Mater. Des. 108 (2016) 632-639. https://doi.org/10.1016/j.matdes.2016.06.104.

[65] Santos, R.A.S., M.J. Campagnole-Santos, and S.l.P. Andrade. Angiotensin-(1–7): an update, Regul. Pept. 91 (2000) 45-62. https://doi.org/10.1016/S0167-0115(00)00138-5.

[66] Suzuki, Y., M. Ruiz-Ortega, O. Lorenzo, M. Ruperez, V. Esteban, and J. Egido. Inflammation and angiotensin II, Int. J. Biochem. Cell Biol. 35 (2003) 881-900. https://doi.org/10.1016/S1357-2725(02)00271-6.
[67] Wang, Y., et al. Higher Concentration of Adrenocorticotropic Hormone Predicts Post-Stroke Depression, Clin. Interv. Aging. 17 (2022) 417-427. https://doi.org/10.2147/CIA.S356361.

The authors declare that they have no known competing financial interests or personal relationships that could have appeared to influence the work reported in this paper.